CFD simulation of pollutant dispersion in a street canyon: Impact of idealized and realistic sources

Peng Qin[1*], *Alessio* Ricci[1,2], and *Bert* Blocken[3]

[1]Department of the Built Environment, Building Physics and Services, Eindhoven University of Technology, Eindhoven, The Netherlands
[2]Department of Science, Technology and Society, University School for Advanced Studies IUSS Pavia, Piazza della Vittoria 15, 27100, Pavia, Italy
[3]Department of Civil Engineering, Building Physics and Sustainable Design, KU Leuven, Leuven, Belgium

Abstract. Pollutant dispersion is of great relevance for people living in urban areas. High levels of pollutant can usually result from the combination of poor natural ventilation and high-traffic volumes of vehicles. Idealized point and line sources are commonly used to reproduce traffic emissions in simplified portions of urban areas, as street canyons. However, a limited number of studies focuses on the usage of realistic sources, as real car geometries which can influence the flow characteristics and the pollutant distribution inside the canyon. This is also the goal of the present paper for which Computational Fluid Dynamics (CFD) simulations were performed by means of scale-adaptive simulation (SAS) on a street canyon to investigate the impact of idealized and realistic sources. In *stage 1*, SAS simulations were performed with idealized line sources by reproducing reduced-scale wind-tunnel (WT) experiments. In *stage 2*, SAS simulations were carried out on a street canyon using idealized line sources and realistic sources with different levels of simplification. The results showed that the use of realistic sources can result in an increased concentration of 1.03 - 6.76 (at z = 0.33 m above the ground), with respect to the use of idealized line sources. Overall, at the lower level of the street canyon (e.g. z < 1.5 m), the concentration can be strongly affected by the presence of the car bodies. The results of the present study are expected to help urban planners as well as governmental institutions to reduce pollutant concentrations in the street canyon.

1 Introduction

The world is experiencing a gradual increase of population with significant rural-urban area transformations. Streets and squares are generally the main zones of urban areas where human activities take place but also where pollutants are present with high levels of pollutant concentration. However, such high levels can usually result from the combination of poor natural ventilation and high-traffic volumes of vehicles as well as industry smokestacks that may cause serious health problems to human beings. Idealized point sources and line sources are commonly used by the Wind Engineering (WE) community to numerically (e.g. by Computational Fluid Dynamics, CFD) and experimentally (e.g. by wind-tunnel, WT) reproduce the traffic emission of vehicles, in order to investigate the pollutant dispersion in cities or in limited and simplified portion of it, like single or multiple street canyons [e.g. 1]. However, a limited number of studies focuses on the investigation of pollution concentration fields in street canyons generated by realistic sources, as real car geometries or derived simplifications. If on one hand, the approximation from "real" to "ideal" source simplify substantially the work of researchers; on the other hand the presence of the car geometry makes the flow field around the body more turbulent with a potential impact on the pollutant concentration. This is also the goal of the present paper for which SAS simulations were carried out on a street canyon to investigate the impact of idealized and realistic sources. For the realistic source the *DrivAer* model was used. The *DrivAer* is an open-source car model firstly introduced by Heft et al. [2] in a cooperation among the Technical University of Munich, Audi and BMW. In *stage 1*, the SAS simulations were performed with idealized line sources by reproducing the reduce-scale wind-tunnel experiments of Gromke and Ruck [3]. In *stage 2*, four cases using idealized line sources and realistic sources with different levels of simplification were simulated.

The current paper is organized as follows: Section 2 describes the methodology; Section 3 discusses the results of the two stages; Section 4 closes the paper with conclusions and perspectives.

2 Methodology

2.1 *Stage 1*: The validation case

In *stage 1*, a single street canyon with four idealized line sources was simulated by SAS in order to reproduce the

* Corresponding author: p.qin@tue.nl

WT experiments carried out by Gromke and Ruck [3]. The present stage was used basically to validate the numerical settings then adopted in *stage 2*.

The WT tests were conducted in an open-circuit atmospheric boundary layer (ABL) WT with a cross-section of 1 (height) × 2 (width) m^2 at the Karlsruhe Institute of Technology, Germany. The dimensions of the street canyon were 0.12 (W) × 0.12 (H) × 1.2 (L) m^3, with an aspect ratio (W/H) of 1. The sulfur hexafluoride (SF6) was selected as the tracer gas and released from four-line sources mounted on the ground. The dimensions of each line source are 1.42 × 0.003 m^2. The approach ABL wind was generated by means of spires, trip and roughness elements. An electron capture detector (Meltron LH 108) was used to measure the near-wall mean concentration in the street canyon. Results in terms of normalized concentration (C^+) were calculated with Equation 1:

$$C^+ = \frac{CU_H H}{Q/L} \tag{1}$$

where C is the measured mean concentration, U_H is the reference wind speed at the building height (H), and Q/L is the emission rate of tracer gas per unit length.

The computational domain was constructed to accurately reproduce the WT flow conditions (Fig. 1). The height and width of the domain were set to replicate the WT cross-section (1 × 2 m^2). The upstream (from inlet to canyon) and downstream (from canyon to outlet) distances were set to 5H and 15H according to the best practice guidelines for CFD in urban physics [e.g. 4-5]. A grid-sensitivity analysis (GsA) was performed with three different levels of refinement: *coarse* (about 2.5 million cells), *medium* (about 5.5 million cells) and *fine* (about 9.3 million cells). For sake of brevity the GsA results are not reported in this paper. The three grids were simulated with the SAS approach coupled with SST *k-ω* turbulence model. For the inflow conditions, the profile of mean wind speed (U) measured in the WT was used, and the turbulent kinetic energy (k) profile was calculated based on the standard deviation (σ) of U. The turbulent dissipation rate (ε) was calculated with Equation 2:

$$\varepsilon(z) = \frac{u_{ABL}^{*3}}{\kappa(z + z_0)} \tag{2}$$

where the u^*_{ABL} is the friction velocity, z_0 is the aerodynamic roughness length and κ is the von Karman constant assumed equal to 0.42. Note that, the u^*_{ABL} (0.59 m/s) and z_0 (0.004 m) were obtained from the logarithmic law curve fitting of U. Since the hybrid steady-transient SAS approach was used, the vortex method was adopted as inflow generator to perturbate the wind flow field. At the top, side and bottom faces of the domain no-slip wall conditions were imposed. The zero-static gauge pressure was imposed at the outlet face. Second-order discretization schemes were used for both the convection and the viscous terms of the governing equations. The PISO algorithm was adopted for SAS with a time-step size of 0.0003 s. This time-step size was defined to make the Courant-Friedrichs-Lewy (CFL) number less than 1. Ten inner iterations were computed within each time step.

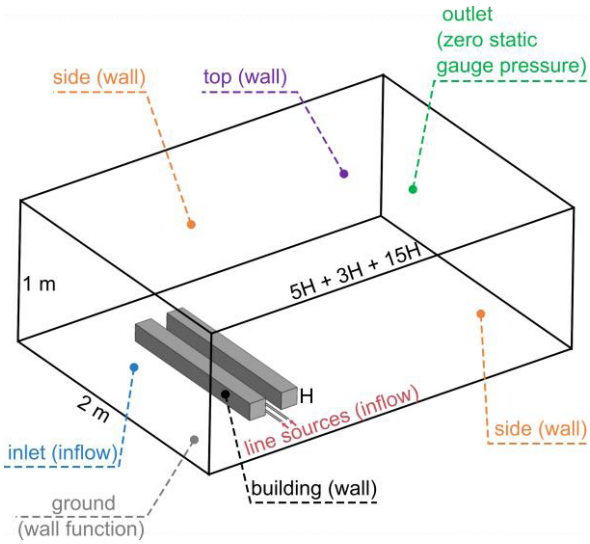

Fig. 1. Computational domain and indication of boundary conditions.

2.2 *Stage 2*: Impact of idealized and realistic sources

In *stage 2*, the domain was built in order to reproduce full-scale dimensions of the canyon (i.e. H = 18 m) and the grid was constructed based on the GsA results of *stage 1*. Four cases were simulated to investigate the impact of idealized sources and realistic sources with different levels of refinement: (*a*) two idealized line sources (ILS) positioned on the ground; (*b*) multiple idealized point sources (MIPS) positioned on the ground (i.e. as a discretization of case *a*); (*c*) multiple idealized point sources ($MIPS^+$) reproducing the exhaust pipes above the ground but without car (*DrivAer*) bodies; (*d*) multiple realistic (*DrivAer*) car sources (MRCS) with (*DrivAer*) car and exhaust-pipe geometries explicitly modeled. The four grids are reported in Figure 2. The carbon monoxide (i.e. CO), one of the most adverse components of car exhaust for humans, was selected as the tracer in the present stage. The total CO emission rate (Q_{total}) for ILS, MIPS, MIPS+ and MRCS was defined based on the Bureau of Science and Technology Standards (BSTS) [6] and set equal to 6.80e-5 kg/s. At the inlet face, the U and k profiles were calculated with Equations 3-4:

$$U(z) = \frac{u_{ABL}^*}{\kappa} ln(\frac{z + z_0}{z_0}) \tag{3}$$

$$k(z) = \frac{{u_{ABL}^*}^2}{\sqrt{C_\mu}} \tag{4}$$

where C_μ (0.09) is the model constant. The same boundary conditions of *stage 1* were used here for the outlet and the bottom surfaces, while at the top and side faces the symmetry condition was imposed. The same solver settings of *stage 1* were also used in *stage 2*, while a time-step size of 0.1 s was adopted for the four cases.

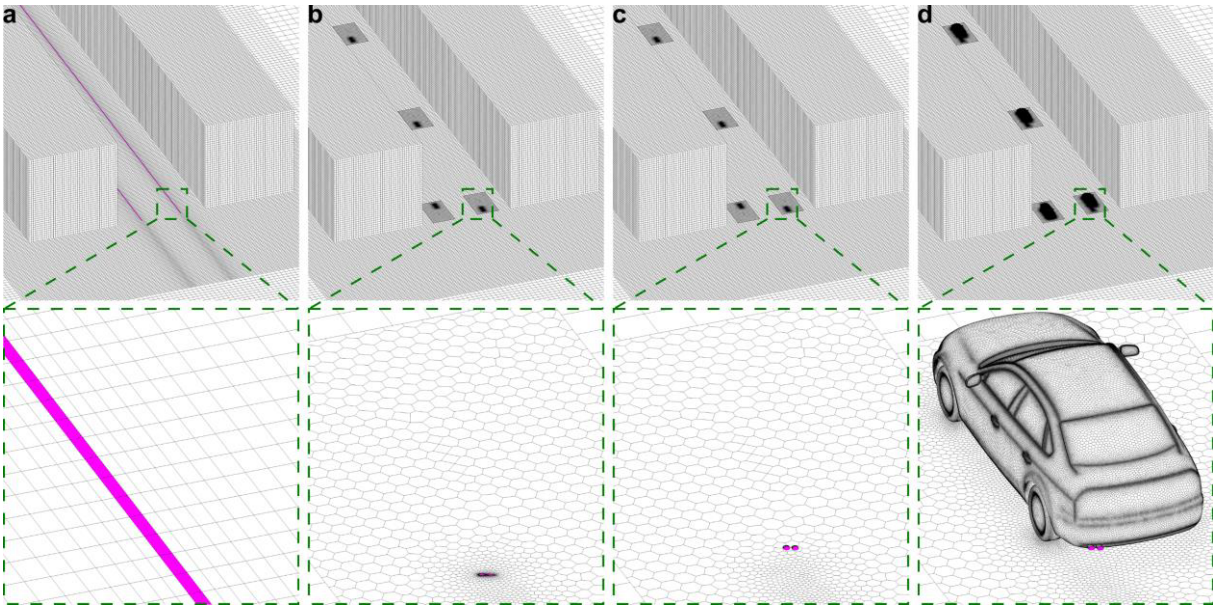

Fig. 2. Computational grids of the four CFD cases: (*a*) idealized line sources (ILS) positioned on the ground; (*b*) multiple idealized point sources (MIPS) positioned on the ground (i.e. as a discretization of case a); (*c*) multiple idealized point sources (MIPS$^+$) reproducing the exhaust pipes above the ground but without car bodies; (*d*) multiple realistic car sources (MRCS) with car and exhaust-pipe geometries explicitly modeled.

3 Results

In *stage 1*, the comparison of SAS and WT results in the street canyon in terms of C^+ was made along vertical lines at $y/H = 0$ and $y/H = 1.25$ near the leeward wall (LW) and windward wall (WW), as shown in Figure 3. In Figure 3, the horizontal and vertical axes indicate the C^+ and z/H; the orange lines and scattered points represent the SAS results obtained in the present study and the WT results obtained from the WT testing [3], respectively; the error bar indicates the measurement uncertainty as reported in Gromke et al. [7].

Near the LW, the average absolute differences of C^+ between SAS and WT at the two lines (i.e. $y/H = 0$ and 1.25) are found to be equal to 3.2 (Fig. 3a) and 0.8 (Fig. 3b), respectively. Near the WW, the average absolute differences of C^+ between SAS and WT at the two lines are found to be equal to 1.1 (Fig. 3c) and 0.5 (Fig. 3d), respectively. Overall, the SAS shows a satisfactory agreement with WT data throughout the monitored lines.

In *stage 2*, the comparison in terms of C^+ contours are made at plane $z = 0.331$ m for the four SAS cases (ILS, MIPS, MIPS$^+$, MRCS) (Fig. 4). In general, the following observations are made:

- Larger C^+ values are observed near the LW (than with respect to the WW), due to the presence of the vortex recirculation positioned nearby.
- Larger C^+ values are found close to the source locations for MIPS (Fig. 3b) than ILS (Fig. 4a).
- A similar C^+ distribution is observed for MIPS (Fig. 4b) and MIPS$^+$ (Fig. 4c), although larger C^+ values (red) are locally found for MIPS$^+$.
- A similar C^+ distribution is observed for MIPS$^+$ (Fig. 4c) and MRCS (Fig. 4d). However, differences are clearly found close to cars when the car geometries are explicitly modeled.

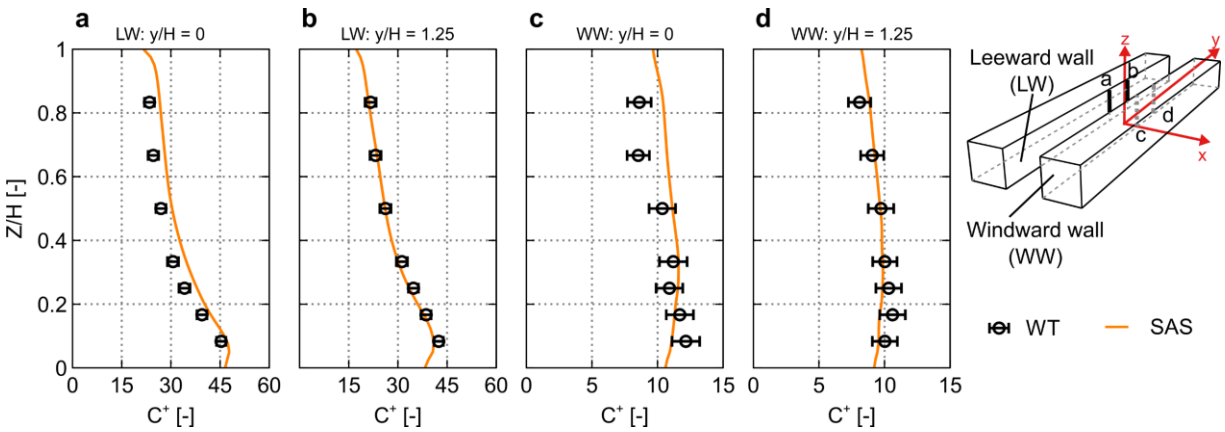

Fig. 3. Comparison of SAS and WT results in terms of C^+ along vertical lines at $y/H = 0$ and 1.25 near the (a, b) leeward wall (LW) and (c, d) windward wall (WW).

Therefore, it can be inferred that the source height may be one of the reasons causing deviations in terms of C^+ values between MIPS and MIPS$^+$. The use of MRCS will lead to generally higher C^+ values in the street canyon (e.g. at z = 0.331 m), with respect to the use of ILS, MIPS and MIPS$^+$.

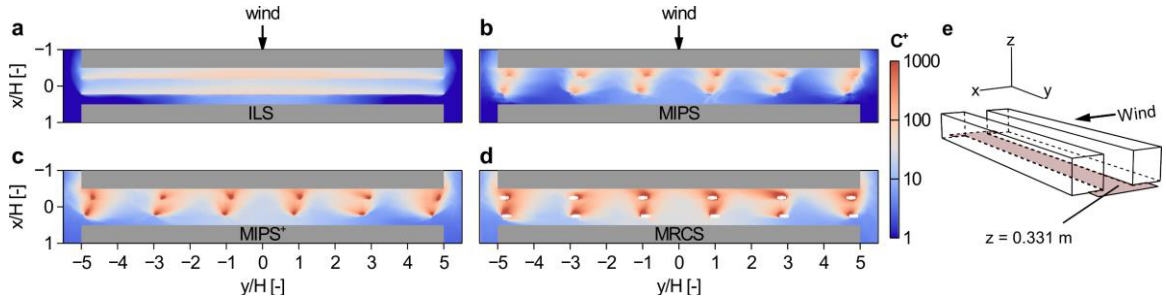

Fig. 4. Comparison of C+ contours made at the plane z = 0.331 m for the four SAS cases: (a) ILS, (b) MIPS, (c) MIPS$^+$ and (d) MRCS. (e) Indication of the horizontal plane (i.e. z = 0.331 m) used for the contours.

Figure 5 shows the plane-averaged C^+ ($<C^+>$) over the plane z = 0.331 m for the four SAS cases. The $<C^+>$ is defined as follows by Equation 5:

$$\langle C^+ \rangle = \frac{\int_A C^+ dA}{A} \tag{5}$$

where A is the plane area at z = 0.331 m (Fig. 4e), equal to 3888 m^2. In Figure 5, the horizontal and vertical axes show the SAS cases (i.e. ILS, MIPS, MIPS+ and MRCS) and the $<C^+>$, respectively. The impact of different sources on the $<C^+>$ is quite evident. The use of realistic sources with different levels of simplification (i.e. MIPS, MIPS+, MRCS) can result in an increase of 1.03 - 6.76 of $<C^+>$ (at z = 0.331 m), with respect to the use of idealized sources (i.e. ILS).

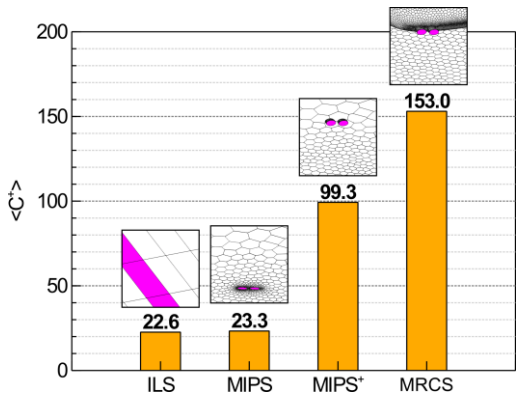

Fig. 5. Plane-averaged C^+ ($<C^+>$) over the plane z = 0.331 m for the four SAS cases.

4 Conclusions and perspectives

In this paper the pollution concentration in a street canyon was assessed by using idealized and realistic sources. In the validation study (i.e. *stage 1*) the SAS model approach was found to perform well and for this reason was selected for the analyses of *stage 2*. In *stage 2*, the SAS results showed that the usage of MRCS can have a significant impact on C^+ distribution near the source location, compared to ILS, MIPS and MIPS+. The use of realistic sources with different levels of simplification (i.e. MIPS, MIPS$^+$, MRCS) can result in an increase of 1.03 - 6.76 of $<C^+>$ with respect to the use of idealized line sources (ILS). Overall, the concentration at the lower level of the street canyon (e.g. z < 1.5 m) can be strongly affected by the presence of the car bodies. Future investigations will focus on the combined effects of realistic sources and vegetation on pollutant dispersion, in order to find optimal vegetation layouts to alleviate the pollution problem in the street canyon. The results of the present study are expected to help urban planners as well as governmental institutions to reduce pollutant concentrations in the street canyon.

References

1. Y. Zhao, L.W. Chew, A. Kubilay, J. Carmeliet, Isothermal and non-isothermal flow in street canyons: A review from theoretical, experimental and numerical perspectives, Build. Environ. **184** (2020) 107163.
2. A.I. Heft, T. Indinger, N.A. Adams, Introduction of a new realistic generic car model for aerodynamic investigations, in: SAE Tech. Pap., SAE International, (2012).
3. C. Gromke, B. Ruck, On the Impact of Trees on Dispersion Processes of Traffic Emissions in Street Canyons, Bound -Layer Meteorol. **131** (2009) 19–34.
4. Y. Tominaga, A. Mochida, R. Yoshie, H. Kataoka, T. Nozu, M. Yoshikawa, T. Shirasawa, AIJ guidelines for practical applications of CFD to pedestrian wind environment around buildings, J. Wind Eng. Ind. Aerodyn. **96** (2008) 1749–1761.
5. B. Blocken, Computational Fluid Dynamics for urban physics: Importance, scales, possibilities, limitations and ten tips and tricks towards accurate and reliable simulations, Build. Environ. **91** (2015) 219–245.
6. Bureau of Science and Technology Standards (BSTS), Technical Guidelines for the Compilation of Air Pollutant Emission Inventory for Road Motor Vehicles, (2015) 26–49.
7. C. Gromke, Einfluss von Bäumen auf die Durchlüftung, 2008.